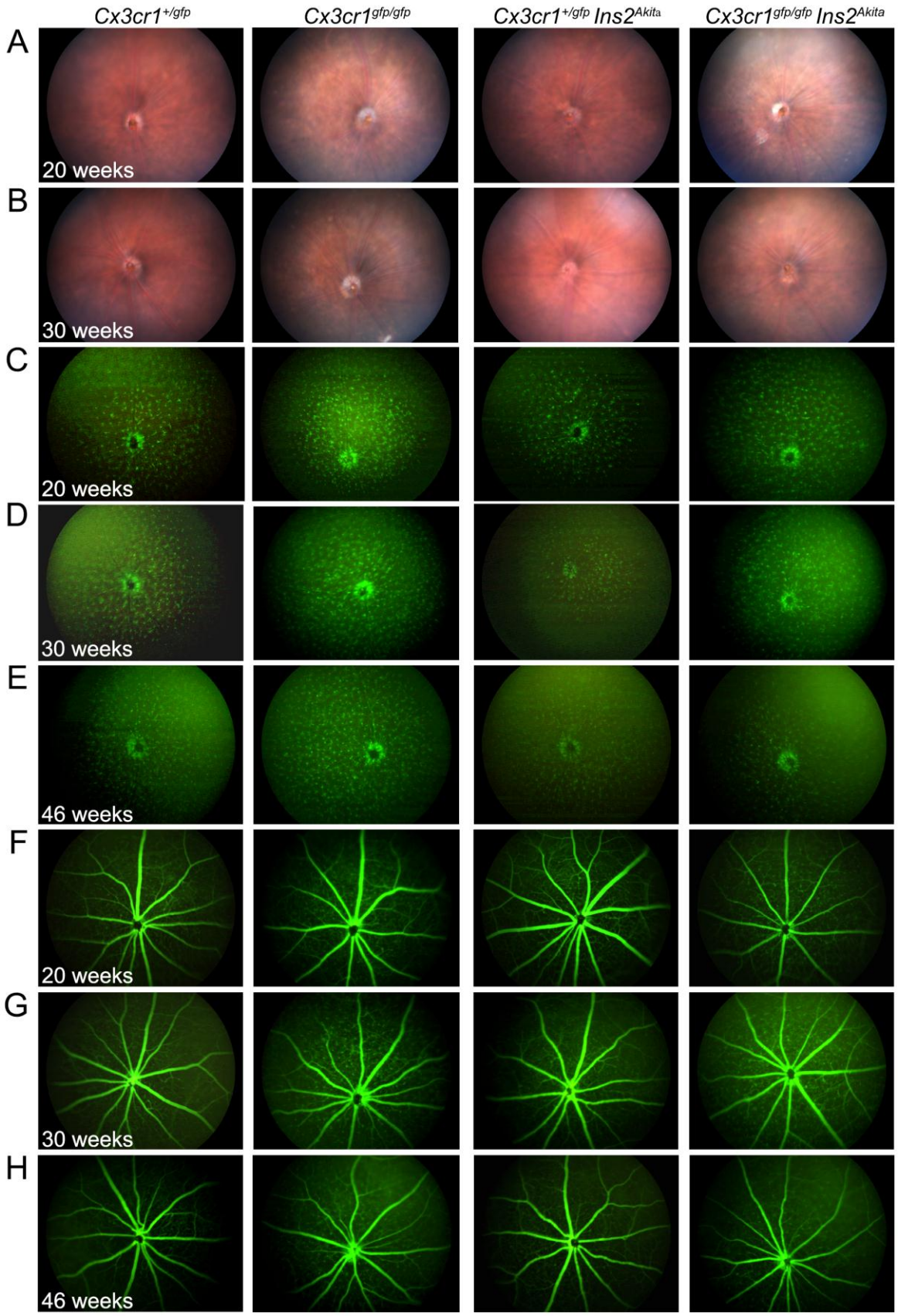
Cx3cr1+/gfp
Cx3cr1gfp/gfp
Cx3cr1+/gfp Ins2Akita
Cx3cr1gfp/gfp Ins2Akita
A
20 weeks
B
30 weeks
C
20 weeks
D
30 weeks
E
46 weeks
F
20 weeks
G
30 weeks
H
46 weeks

Supplementary Figure 1: *In vivo* retinal imaging

Clinical assessment of non-diabetic (*Cx$_3$cr1$^{gfp/+}$* and *Cx$_3$cr1$^{gfp/gfp}$*) and diabetic (*Cx$_3$cr1$^{gfp/+}$ Ins2^{Akita}* and *Cx$_3$cr1$^{gfp/gfp}$ Ins2^{Akita}*) mice using the Micron III retinal imaging system. Images are representative snapshots extracted from 20 second videos. Brightfield assessment of the mouse fundus at 20 weeks (A) and 30 weeks (B) of age revealed no overt changes associated with hyperglycemia or Cx$_3$cr1 deficiency. Fluorescence examination of the mouse fundus at 20 weeks (C), 30 weeks (D) and 46 weeks (E) of age revealed no changes to the normal distribution of retinal microglia. No vascular leakage was detected by fluorescein angiography at 20 weeks (F), 30 weeks (G) or 46 weeks (H) of age.

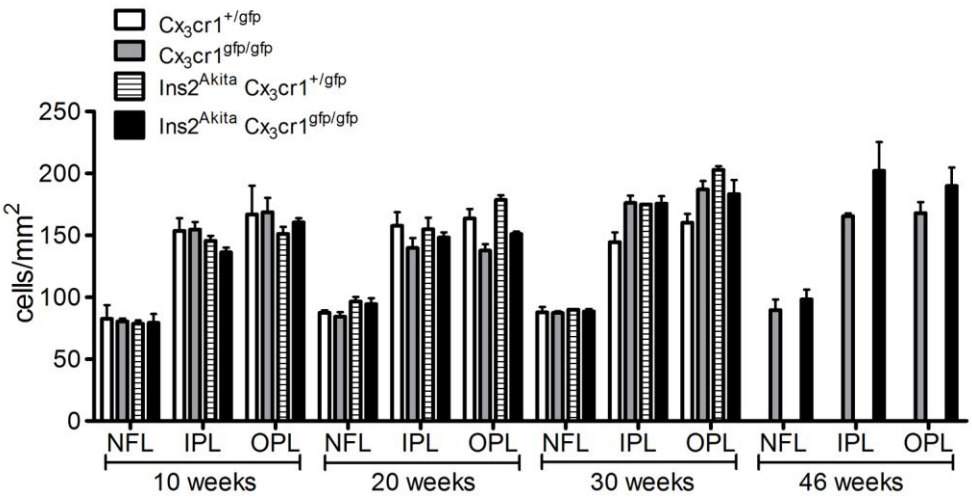

Supplementary Figure 2: Retinal microglial cell numbers in the NFL, IPL and OPL of *Ins2*^{Akita} mice

Quantitative analysis of microglia residing in the nerve fiber layer (NFL), inner plexiform layer (IPL) and outer plexiform layer (OPL) revealed no significant differences in cell densities between non-diabetic and diabetic mice at all time points examined (D).

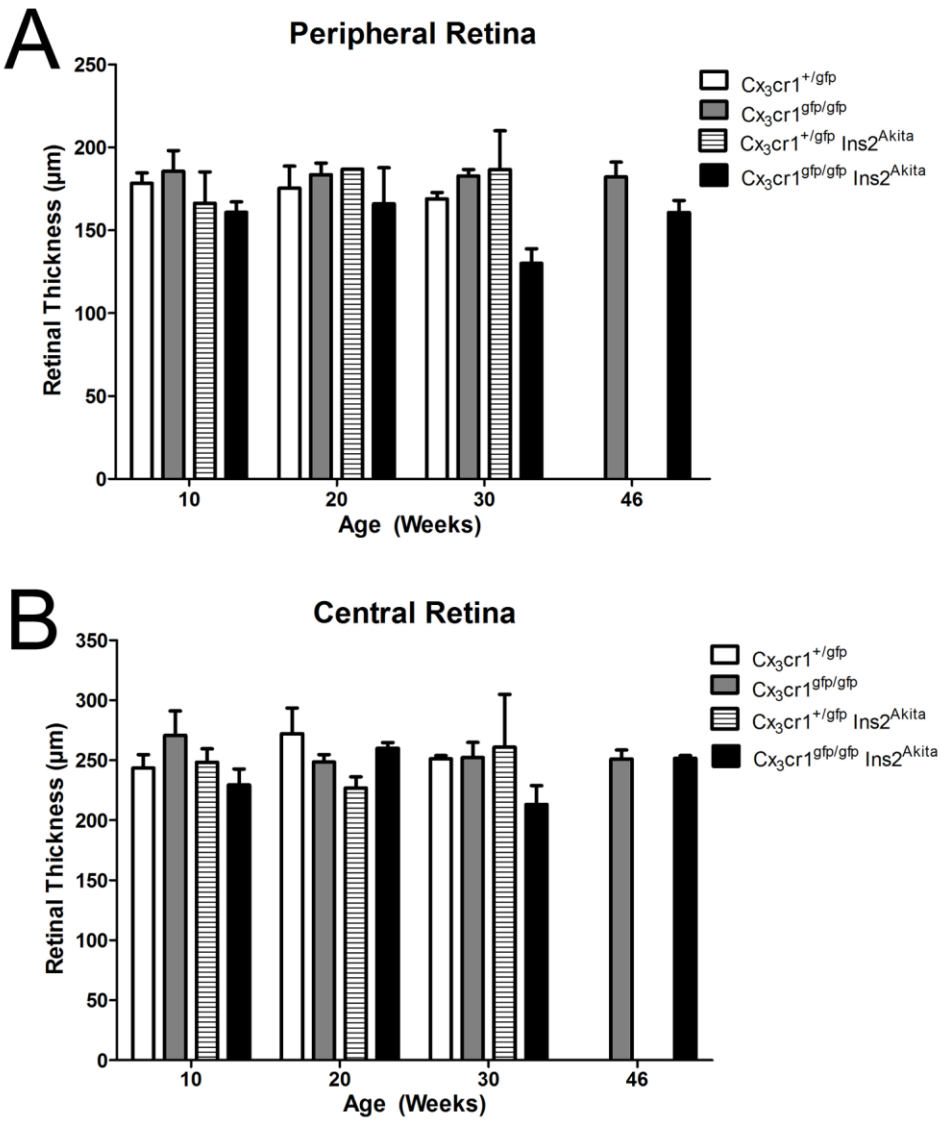

Supplementary Figure 3: Peripheral and central retinal thicknesses in *Ins2*^{Akita} mice

Peripheral (A) and central (B) retinal thicknesses measured from GMA-embedded eye sections of non-diabetic (*Cx*$_3$*cr1*$^{gfp/+}$ and *Cx*$_3$*cr1*$^{gfp/gfp}$) and diabetic (*Cx*$_3$*cr1*$^{gfp/+}$ *Ins2*^{Akita} and *Cx*$_3$*cr1*$^{gfp/gfp}$ *Ins2*^{Akita}) mice at 10, 20, 30 and 46 weeks of age. Cx$_3$cr1-deficiency and diabetic status did not alter peripheral or central retinal thickness.

Supplementary Video 1: 3D visualization of the retinal microglial network in a 30 week old *Cx$_3$cr1$^{gfp/gfp}$* mouse

Confocal microscopy was used to generate a whole retinal scan from the nerve fiber layer (top) to photoreceptor cell layer (bottom). A 3D video was created using Imaris Software in order to more closely visualize microglial networks in the inner plexiform layer (IPL) and outer plexiform layer (OPL). Note GFP$^+$ IPL and OPL microglia reside in regular, distinct networks, with few cell processes extending into the inner nuclear layer (represented by the distinct band in between the IPL and OPL).

Supplementary Video 2: 3D visualization of the retinal microglial network in a 30 week old *Cx$_3$cr1$^{gfp/gfp}$ Ins2^{Akita}* mouse

Confocal microscopy was used to generate a whole retinal scan from the nerve fiber layer (top) to photoreceptor cell layer (PCL; bottom). A 3D video was created using Imaris Software in order to more closely visualize microglial networks in the inner plexiform layer (IPL) and outer plexiform layer (OPL). The GFP$^+$ microglial architecture in the IPL and OPL is disrupted, with numerous cell processes extending into the inner nuclear layer (INL). Note the presence of numerous GFP$^+$ cells in the PCL, representative of subretinal macrophage accumulation.